THE JOURNAL OF PHYSICAL CHEMISTRY B

Article

pubs.acs.org/JPCB

Quantitative Determination of Ala-Ala Conformer Ratios in Solution by Decomposition of Raman Optical Activity Spectra

Jakub Jungwirth,[†,‡] Jaroslav Šebestík,[†] Martin Šafařík,[†] Josef Kapitán,[*,§] and Petr Bouř[*,†]

[†]Institute of Organic Chemistry and Biochemistry, Academy of Sciences, Flemingovo náměstí 2, 16610 Prague, Czech Republic

[‡]Faculty of Mathematics and Physics, Charles University, Ke Karlovu 3, 12116 Prague, Czech Republic

[§]Department of Optics, Palacký University, 17. listopadu 12, 77146 Olomouc, Czech Republic

Supporting Information

ABSTRACT: Raman optical activity (ROA) spectroscopy combined with quantum-chemical simulations is a sensitive method to determine the absolute configuration and conformation of chiral molecules in solutions. However, the precision of this approach varies for different systems. In the present study, the reliability and numerical stability of decomposing experimental spectra into calculated subspectra is tested on the Ala-Ala dipeptide. Molecular dynamics (MD) snapshots of Ala-Ala/water clusters are averaged to account for solvent effects and molecular flexibility. Multiple experiments with protonated, zwitterionic, and deprotonated dipeptide forms and natural and d_2- and d_8-isotopically labeled dipeptides are used to verify the results and estimate the overall accuracy. Although the precision is still limited by experimental noise and computational error, a very close match between the observed and theoretical spectral shapes has been achieved. This enabled quantitative determination of conformer populations with a typical dispersion of 10%. The spectroscopy also demonstrated how the conformation depends on pH. The ROA results were more consistent than the Raman ones. Typically, the ROA analysis was more resistant to artifacts in the experiment, such as incomplete baseline subtraction. Conformer ratios predicted by MD agree fairly but not fully with the experimental ones. This indicates minor deficiencies in the Amber force field, particularly for the protonated dipeptide. Overall, the combination of ROA experiment and computational chemistry appears to be a robust tool providing deep insight into molecular structure.

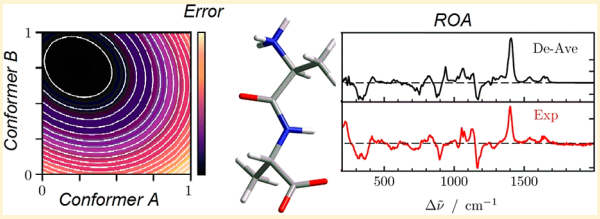

INTRODUCTION

The conformational behavior of small peptides has been attracting attention because of its relation to their biological activity and to protein folding in general. However, there are a limited number of methods applicable to studying molecules in solutions. In this respect, Raman optical activity (ROA) spectroscopy established itself as a very helpful tool. It is particularly suited for the native aqueous environment because the Raman background signal of water is relatively weak and does not interfere much with that of the studied compounds. ROA spectrometers measure both the total (Raman) and differential scattering of right and left circularly polarized light.[1−3] ROA spectra thus provide additional information about molecular chirality (absolute configuration). However, also fine conformational changes usually bring about bigger changes in ROA spectra than for Raman. So far, the chiral technique has been applied to a wide range of biologically relevant systems, such as sugars, peptides, and nucleic acids.[4−9]

The potential of ROA has been further boosted by the possibility to reliably simulate ROA intensities.[10] Efficient implementations of density functional theory (DFT)[11−14] made it possible to interpret the spectra without empirical premises. Computer parallelization,[15] fragment-based ab initio methods,[16] or Cartesian tensor transfer techniques[17,18] made such accurate spectral simulations applicable even to very large molecules.

Still, the accuracy of simulated vibrational band frequencies and intensities varies across systems, which limits the knowledge that can be obtained about molecular structure from a spectroscopic experiment. In particular, spectra of polar and flexible molecules that are highly relevant to biology need to be simulated by relatively complex, combined molecular mechanics/quantum mechanics (MM/QM) procedures.[19,20] Visual comparison of simulated and experimental spectra or a direct decomposition of the experimental spectra into simulated ones are then used to reveal conformer ratios in the sample.[21−23] However, as far as we know, the practical accuracy and numerical stability of such a procedure for flexible molecules have not been extensively tested yet.

In the present work, a combined theoretical and experimental approach is used to study the conformational behavior of such a "difficult" system, the Ala-Ala dipeptide. This is an important model for proteins, as their spectra largely depend on short-range interactions between adjacent amino acid units along the main peptide chain.[18,24−26] Apart from a natural dipeptide, "d_2" and "d_8" deuterated species were synthesized and their spectra also measured and analyzed. Such labeling with stable isotopes has been used as an excellent

Received: July 20, 2017
Revised: August 29, 2017
Published: August 30, 2017

ACS Publications © 2017 American Chemical Society

DOI: 10.1021/acs.jpcb.7b07154
J. Phys. Chem. B 2017, 121, 8956−8964

way to assign vibrational bands and monitor the signal and structure of specific molecular parts.[27−30] Deuteration leaves the electronic structure nearly unaltered, and its effect on the Ala-Ala conformation is negligible. Conformer ratios obtained with different isotopically labeled species should be equal, and actual values thus help to verify the reliability of the method as such.

The Ala-Ala molecule has been previously studied as a convenient model of the peptide linkage.[27,31−33] However, its conformational behavior still remains to be clarified. For example, quantum-chemical methods cannot be applied directly to the zwitterionic form not stable in a vacuum.[34] Coexistence of the NH_3^+ and COO^- groups in such a small system must be stabilized by polar solvent. In a way, flexible peptides are more complicated for modeling than larger ones where only a limited number of standard conformations are stabilized by side chain interactions.[35] In a crystal, Ala-Ala exists in the zwitterionic form;[36] its conformation nevertheless changes when dissolved in water, and is pH dependent.[37] Previous simulations of ROA spectra did provide valuable information on Ala-Ala conformational behavior[38−42] but were not accurate enough to provide meaningful experimental conformer ratios using decomposition/fit algorithms.

Another interesting question is whether the ROA spectra are better suited than the Raman ones to be decomposed into individual components. This is a principal issue for the ROA technique aimed to provide better structural sensitivity than unpolarized Raman spectroscopy. Although the ROA bands are inherently more sensitive to the structure, recent analysis of sugar mixtures[43] showed that artifacts and ROA intensity noise, roughly proportional to the square root of the total Raman signal,[3] can make the ROA analysis less reliable. For Ala-Ala, it turns out that the decomposition efficiency is for both spectral kinds roughly the same, or even favoring ROA.

METHODS

Sample Preparation and Spectra Measurement. Natural L-Ala-L-Ala (Ala-Ala) peptide was obtained from Sigma-Aldrich, while deuterated L-Ala-d_1-L-Ala-d_1 and L-Ala-d_4-L-Ala-d_4 molecules (Figure 1) were synthesized from isotopically labeled alanine (Sigma-Aldrich) according to an established procedure.[44] Details about the synthesis and compound characterization are summarized in the Supporting Information. Backscattered Raman and ROA spectra were recorded on a scattered circular polarization (SCP) BioTools μ-ChiralRAMAN-2X instrument[1,45] at Inst. Org. Chem. Biochem. (Prague), using 532 nm laser excitation. Control measurements were carried out on a similar but custom-made instrument at Palacký University (Olomouc). No significant differences between the experimental results were observed. The peptides were dissolved in water to concentrations of 100 mg/mL. For the charged forms, the pH was adjusted by HCl (to 1.3) or NaOH (to 12.0). The laser power at the sample was 330−560 mW, and the acquisition time was 12−33 h. The samples were measured in a rectangular fused silica cell at room temperature (~298 K). The Raman spectrum of the cell filled with the solvent was subtracted from all Raman spectra. ROA spectra were corrected by a polynomial baseline. The frequency scale was calibrated using a neon lamp, and the intensity calibrated with a standard fluorescence reference material 2242 (National Institute of Standards and Technology, USA).

Molecular Dynamics Simulations. The protonated, zwitterionic, and deprotonated dipeptides were separately

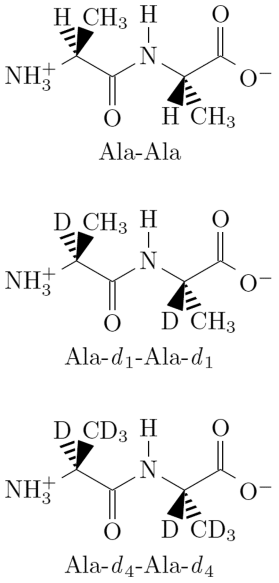

Figure 1. Zwitterionic forms of the natural and two isotopically labeled Ala-Ala species.

placed in a cubic box (30 Å a side) filled with water molecules. After 1 ns equilibration, productive MD was run for another 1 ns with the Amber10[46] software using the Amber03[47] force field, *NTV* thermodynamic ensemble, a temperature of 300 K, 1 fs integration step, and periodic boundary conditions. Snapshots of the geometry were saved each 1 ps and divided into four classes corresponding to distinct Ala-Ala conformers (**A**−**D**, centered around (φ, ψ_N) values of ~(−155°, 150°), (−70°, 150°), (−155°, −70°), (−70°, −60°), respectively, Scheme 1). In addition to the restraint-free dynamics, the

Scheme 1. Definition of the Principal Torsion Angles

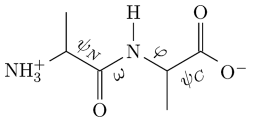

weighted histogram analysis method (WHAM)[48] was used to determine the free energy within the full extent of the ψ_N and φ angles. Only the trans-conformer (ω = 180°) was considered. The simulations were done with the natural ("d_0") peptide; we verified that the deuterations did not change resultant free energies within numerical accuracy.

Computation of Raman and ROA Spectra. For 100 snapshots of each isotopically labeled form ("d_0", "d_2", and "d_8"), each level of protonation (protonated, zwitterionic, and deprotonated), and each conformer (**A**−**D**), spectra were generated within the harmonic approximation. First, water molecules farther than 3.6 Å from the peptide were deleted. Then, the geometries of remaining clusters containing the peptide and 11−17 water molecules were partially optimized in vibrational normal mode coordinates.[49,50] Modes with frequencies lower than 250 cm^{-1} were fixed. This procedure ensured that the MD geometry was approximately conserved, while the vibrational modes most important for the spectra were relaxed.[51] The program Qgrad[50] interfaced to the Gaussian software package[52] was used for the partial optimization. All quantum-chemical computations were performed at the B3PW91/6-311++G** level of theory. The

DOI: 10.1021/acs.jpcb.7b07154
J. Phys. Chem. B 2017, 121, 8956−8964

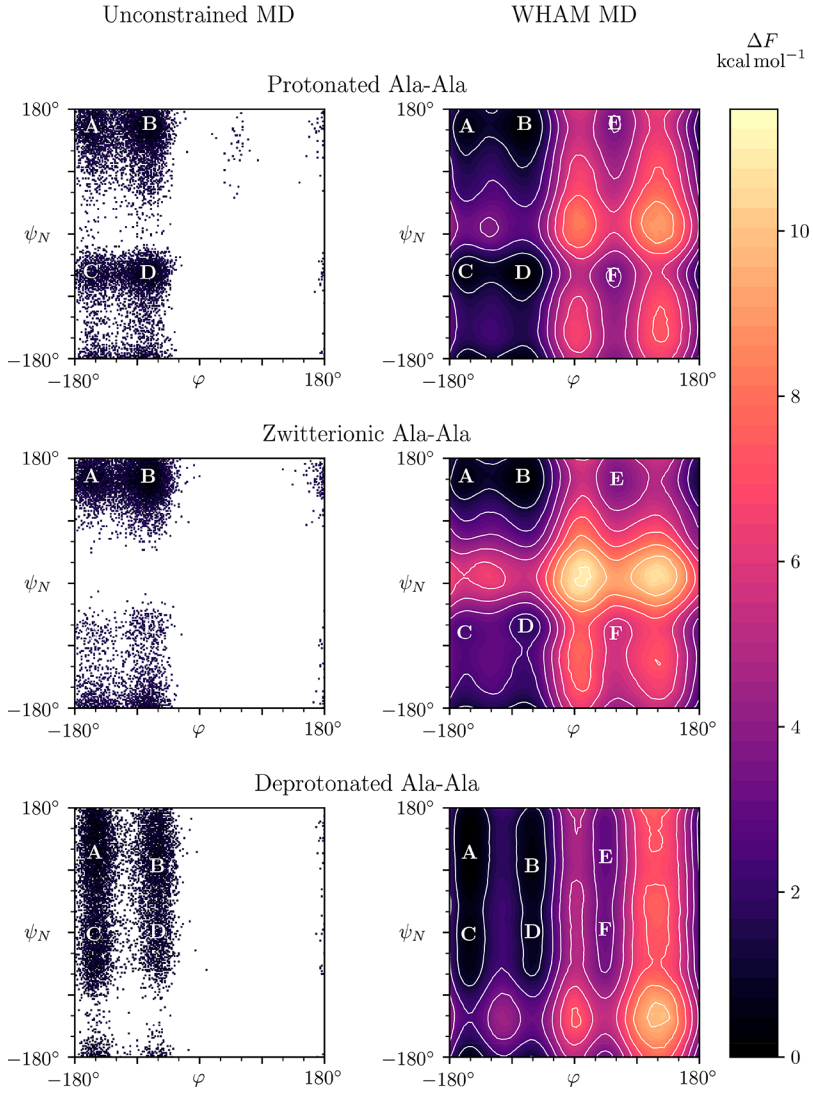

Figure 2. Free energy as a function of φ and ψ_N as obtained from unconstrained (left) and WHAM (right) MD for protonated, zwitterionic, and deprotonated Ala-Ala forms.

solute−solvent clusters were embedded in a dielectric environment accounting for the remaining solvent using the conductor-like polarizable continuum solvent model (COSMO).[53,54] After the optimization, Raman and ROA intensities[2,3,55] were calculated by Gaussian.

Contribution of the water molecules in the clusters was not considered; i.e., the intensity tensors ($\boldsymbol{\alpha}$, $\mathbf{G}'$, and $\mathbf{A}$)[2] were set to zero for the water atoms. This decreased the residual error in the spectra as a larger number of the clusters would be needed to average out the solvent contribution to ROA. At present, we consider direct contribution of the water molecules to sample chirality undetectable; also, computations suggest that the effect on the decomposition results is negligible.

The theoretical spectra ($S(\omega)$) were obtained by convolution of calculated intensities (I_i) with Lorentzian bands including the Boltzmann temperature factor[55] as

$$S(\omega) = \sum_i \frac{I_i}{\omega_i}\left[1 - \exp\left(-\frac{\hbar\omega_i}{kT}\right)\right]^{-1}\left[4\left(\frac{\omega - \omega_i}{\Delta}\right)^2 + 1\right]^{-1} \quad (1)$$

where ω_i is the frequency of transition i, k is the Boltzmann constant, T is the temperature (298 K), and Δ = 10 cm^{-1}. Gaussian provides the intensities in Å^4/m$_u$ (Raman) and Å^5/m$_u$ (ROA), where m$_u$ is the atomic mass unit.

Raman and ROA Spectra Decompositions. Prior to the decomposition itself, the frequency in the calculated spectra was linearly transformed as

$$\omega' = a\omega + b \quad (2)$$

to maximize overlap with experimental spectra and thus correct for a systematic computational error.[55] ω and ω' are the calculated and scaled frequency, respectively, a = 0.969 and b = 19 cm^{-1}. An example of this frequency "scaling" is given in Figure S1 in the Supporting Information. The scaled computed spectra are also presented in the plots.

The experimental spectra (S_{exp}) were supposed to be linear combinations of spectra calculated for individual conformers (S_i), with coefficients c_i obeying

$$\sum_{i=1}^{N} c_i = 1 \quad \text{and} \quad 0 \le c_i \le 1 \quad (3)$$

DOI: 10.1021/acs.jpcb.7b07154
J. Phys. Chem. B 2017, 121, 8956−8964

In our case, $N = 4$ (conformers **A**–**D**). The coefficients were obtained by minimizing the spectral error as a function of the coefficients c_i

$$\delta = \int_{\omega_{min}}^{\omega_{max}} [S_{exp}(\omega) - \sum_{i=1}^{N} c_i S_i(\omega)]^2 \, d\omega \quad (4)$$

where $\omega_{min} = 300$ cm^{-1} and $\omega_{max} = 1900$ cm^{-1}. A direct scan of the N-dimensional coefficient space on a grid was performed to locate the minimum.

The fact that only relative Raman intensities are measured brings about an ambiguity when calculating the error (eq 4). We thus found the minimum for arbitrary positive values of c_i (without the restrictions in eq 3), and the resulting coefficients were normalized to add up to unity afterward. An alternative option to normalize spectral intensities beforehand and then search for the minimum strictly obeying eq 3 was examined too. However, this latter approach performed rather poorly for spectra suffering from fluorescence or other baseline problems, and was thus abandoned.

Unlike the usual minimization algorithms, such as those based on Lagrange multipliers or singular value decomposition, the direct scanning does not require special measures to eliminate negative coefficients. Also, it does not presume any particular property of δ as a function of the coefficients, such as smoothness and uniqueness of the minimum. On the other hand, systematic scanning of the N-dimensional coefficient space is more time-consuming. Fortunately, scanning in coarse steps and refining the result only in the vicinity of the minimum can significantly speed up the process to seconds to minutes of computer time.

RESULTS AND DISCUSSION

Molecular Dynamics and "Conformational Switching" Induced by pH. The distribution of MD snapshots obtained from the free dynamics and WHAM free-energy profiles are plotted in Figure 2. They are consistent with previous MD studies performed mostly on the Ala-Ala zwitterionic form.[56−59] On the other hand, ab initio computations typically provided a rather incomplete description of the zwitterionic conformer behavior (Table S1).[34,39−41,60] Neither vacuum nor the dielectric solvent model alone sufficiently support the hydrogen bonding interactions and separation of charges in the zwitterion.[23,61]

The φ and ψ_N torsion angles of the free energy minima for all three forms are listed in Table S2. The last two columns in the table compare conformer weights obtained by integrating the entire conformer regions with Boltzmann weights on the basis of energies of the minima. It is interesting that these two approaches significantly differ for the protonated form, where the WHAM potential energy surface integration yields 40% of conformer **B**, while the population estimated from the minimum is only 31%. Note that the integration is more reliable, as it better accounts for molecular flexibility and state degeneracy (associated with variations of other coordinates than φ and ψ_N) at a particular point of the φ and ψ_N plane.[62]

Typical conformer geometries close to the free-energy minima are shown in Figure 3. The extended ("**A**") and more puckered ("**B**") conformations respectively correspond to standard β-sheet and polyproline II-like protein secondary structures.[63] The polyproline II conformation is considered to be a good model of the so-called random peptide conformation.[64] In both **A** and **B**, the ψ_N angle is close to

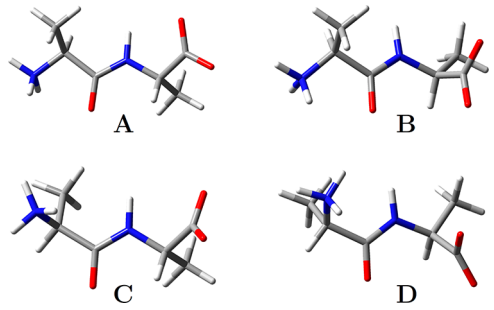

Figure 3. Four most populated conformers of the Ala-Ala zwitterion.

152°, and is stabilized by internal hydrogen bonding between the NH_3^+ group and amide oxygen. **C** does not have a longer polypeptide analogue, and the **D** form is close to standard α- or 3_{10}-helices.[63] The remaining two conformers (**E** and **F**) are not further discussed, as their relative populations were predicted to be small (<1%) and their inclusion resulted in only negligible improvements of the simulated spectra.

Figure 2 also shows that the relative conformer populations are affected by protonation and deprotonation of the dipeptide. In the protonated form, for example, a ψ_N angle of about −57° (assigned to the **C** and **D** conformers) appears more frequently than in the zwitterion. The deprotonation causes a significant increase in molecular flexibility as the ψ_N angle can rotate almost freely between the **A** and **C** or **B** and **D** energy minima. These changes are also reflected in histograms of the angular populations obtained from unconstrained MD simulations (Figure S2). Such pH-induced conformer changes were also predicted for Ala-Ala by NMR.[40]

Experimental versus Calculated Spectra. A detailed analysis of Ala-Ala vibrational transitions can be found in previous studies.[34,39,41,42] Assignment of the most intense Raman peaks can be found in Table S3. Raman and ROA spectra of all four conformers and variously protonated and isotopically labeled dipeptides are plotted in Figure S3. In Figure 4, the experimental spectra of the respective protonated, zwitterionic, and deprotonated forms are compared to the resultant theoretical fit.

As expected, the ROA spectra are much more sensitive to conformational changes (**A**...**D**) than the Raman ones, while the protonation and isotopic labeling are well-reflected in both spectral types. In no case can an individual conformer alone fully explain the experiment. The fit (decomposition) best matches the measured spectra; nevertheless, in most cases, also the methodologically "purer" simulations based on the integrated Boltzmann averaging of the MD snapshots very closely reproduce the measured data (Figures S3). To the best of our knowledge, such a faithful reproduction of Raman and ROA spectra has not been previously achieved for this type of molecule.

Still, there is an occasional mismatch between the simulations and experiment (Figure 4). In the lowest-wavenumber region (<300 cm^{-1}), the experimental Raman spectra may be affected by an incomplete baseline subtraction due to the high water and other background signal. Sample fluorescence was particularly variable in the differently deuterated species and made it difficult to subtract the baseline across the entire spectral region. The experimental ROA spectra were hampered by higher noise (dark current of the CCD camera, intensity "spikes" from cosmic radiation, etc.)[3] and may occasionally exhibit minor artifacts, in particular for weak bands in the

DOI: 10.1021/acs.jpcb.7b07154
J. Phys. Chem. B 2017, 121, 8956−8964

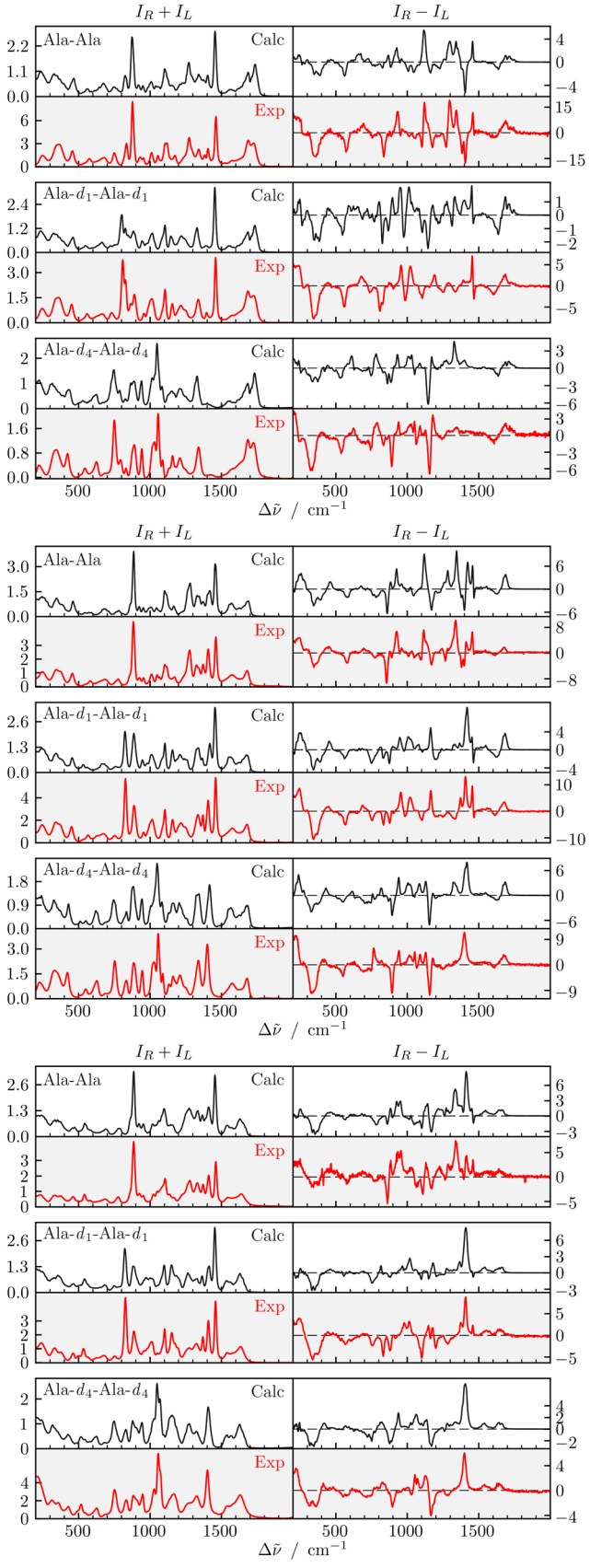

Figure 4. (Top) Protonated isotopic species of Ala-Ala, simulated and experimental (pH 1.3) Raman ($I_R + I_L$) and ROA ($I_R - I_L$) spectra. (Middle) Zwitterionic Ala-Ala dipeptides, simulated and experimental (pH 7) Raman ($I_R + I_L$) and ROA ($I_R - I_L$) spectra. (Bottom) Deprotonated Ala-Ala dipeptides, simulated and experimental (pH 12) Raman ($I_R + I_L$) and ROA ($I_R - I_L$) spectra. The experimental intensities are multiplied by a factor of 10^{-10} (Raman) and 10^{-6} (ROA) to approximately match the calculated scale and avoid large numbers.

vicinity of a strong Raman signal.[65] Overall, however, the spectra are well-reproducible and consistent with older experiments for the nondeuterated (natural) peptide.[42,66]

Another problem affecting the accuracy of the resultant conformer ratios is the limited precision of the simulations. Typically, fine ROA patterns within 800−900 cm^{-1} and around 1300 cm^{-1} are not reproduced. Part of the reason may be the inherent inaccuracy of DFT, as analyzed by extensive benchmark computations.[12,68−70] Although earlier ROA studies indicate a supremacy of the adopted B3PW91 functional,[17,67,12,67−69] trial computations (not shown) reveal that it can still yield different frequency error for different vibrations. This can cause serious distortions of ROA intensities and cannot be corrected unless highly electron-correlated and prohibitively time-consuming computational methods are used.[70,71] Incomplete solvent modeling[72] and anharmonic forces[73,74] not included in the calculations may also contribute to the overall error.

Fortunately, most other spectral features are well-reproduced, including the region below 900 cm^{-1}, rather neglected in the past. The overall good agreement of the experiment and theory thus provides a good basis for a more quantitative analysis of the spectra.

Experimental versus Calculated Conformer Ratios. The decomposition results are summarized in Figure 5 and in Table 1, showing that the coefficients are close but not identical to conformer populations obtained from WHAM. All six independent decompositions (d_0, d_2, and d_8 species for both Raman and ROA spectra) suggest a higher (~70%) content of the **B** conformer ("polyproline II") in protonated Ala-Ala than obtained from the MD (40%). One can interpret this as a bias of the Amber force field toward the **D** "α-helical" conformation. For the zwitterion, the situation is similar, with a smaller difference (~80% vs 67%), while for the deprotonated form a large dispersion of the decomposition coefficients makes such a comparison more difficult.

The decomposition results are somewhat dependent on spectra processing, particularly on the baseline subtraction in Raman spectra and the choice of the analyzed spectral range (ω_{min}, ω_{max}). Jointly with the limited computational accuracy, these factors are responsible for the variation of the decomposition coefficients. For the two spectral kinds and three isotopic species, they typically vary within 5−15%. Overall, the ROA decomposition results seem to be more reliable than the Raman ones, as the coefficients for the three isotopic isomers are more alike, often in surprising agreement (e.g., c_B for the zwitterion, Figure 5 and Table 1). In contrast, decomposition of the Raman spectrum of the deprotonated dipeptide provided 50 and 0% of **D** for the d_2 and d_8 species, respectively. This was, however, to a large extent caused by a close similarity of the Raman spectra of individual conformers, and other cases yielded more consistent results.

Stability of Spectral Decomposition. Next, we investigate the spectral error (δ) as a function of the decomposition coefficients. The uniqueness of the minimum is not self-evident, and we and others often ignored this issue in the

DOI: 10.1021/acs.jpcb.7b07154
J. Phys. Chem. B 2017, 121, 8956−8964

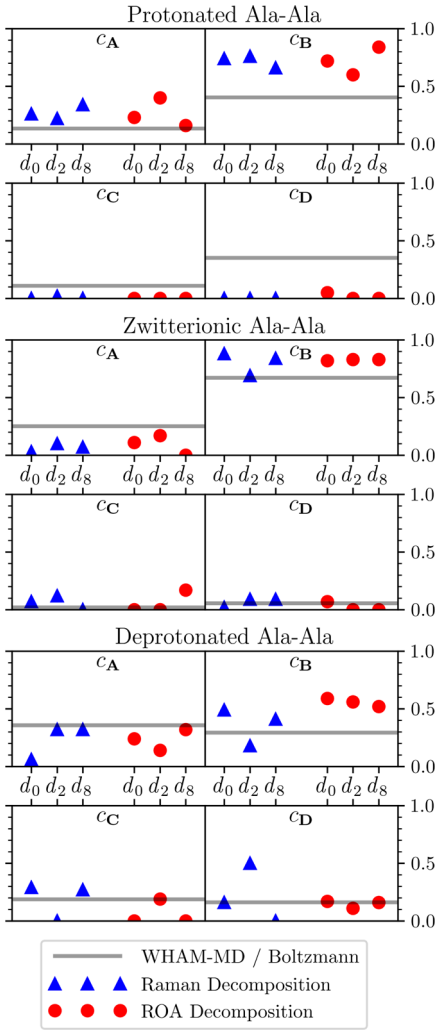

Figure 5. Conformer populations as obtained by the WHAM method (gray line), by the decompositions of Raman (blue triangles) and ROA (red circles) experimental spectra, for three isotopic isomers and three protonation states of Ala-Ala.

Table 1. Boltzmann Weights Calculated by WHAM and Decomposition Coefficients Obtained from Raman and ROA Spectra (%)

	c_A, c_B, c_C, c_D		
deuteration	WHAM	Raman	ROA
	Protonated Ala-Ala		
d_0	13, 40, 12, 35	26, 74, 0, 0	23, 72, 0, 5
d_2		22, 76, 2, 0	40, 60, 0, 0
d_8		34, 66, 0, 0	16, 84, 0, 0
	Zwitterionic Ala-Ala		
d_0	25, 67, 02, 06	3, 88, 7, 2	11, 82, 0, 7
d_2		10, 69, 12, 9	17, 83, 0, 0
d_8		7, 84, 0, 9	0, 83, 17, 0
	Deprotonated Ala-Ala		
d_0	36, 29, 19, 16	6, 49, 29, 16	24, 59, 0, 17
d_2		32, 18, 0, 50	14, 56, 19, 11
d_8		32, 41, 27, 0	32, 52, 0, 16

past.[23,43] Nevertheless, for Ala-Ala, the error has always been a smooth function of the coefficients, with a single minimum. An example of the dependence of normalized δ on two coefficients obtained from spectra of protonated peptide is provided in Figure 6. The dependence additionally justifies searching for minima in coarse steps and refining the result only in the vicinity of the minimum, which significantly speeds up the procedure.

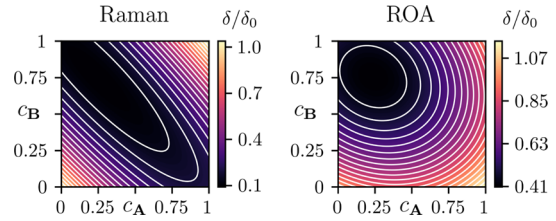

Figure 6. Dependence of the relative spectral error ($\delta_0 = \int_{\omega_{min}}^{\omega_{max}} {S_{exp}}^2(\omega)\, d\omega$) on two coefficients ($c_A$ and c_B) obtained by a decomposition of protonated Ala-Ala Raman and ROA spectra. The remaining coefficients (c_C and c_D) were set to zero.

As δ possesses only one minimum and the function is smooth, the use of analytical approaches is also reasonable. Indeed, an algorithm based on Lagrange multipliers was tested and usually resulted in coefficients that were nearly identical to those obtained by the systematic scan. However, negative decomposition coefficients had to be carefully avoided, a problem affecting ROA more than Raman spectra. For example, penalty functions employed to keep the coefficients positive often caused a significant distortion of the spectral error hypersurface and led to erroneous results. A more viable approach was to set to zero the coefficients that were expected to be negative and reiterate the Lagrange decomposition.

Despite both the Raman and ROA error surfaces being smooth (Figure 6), one should be aware that a variation of the decomposition coefficients causes a much smaller change in the Raman than in the ROA spectra (cf. the individual conformer spectra in Figure S3). This can also be seen from the magnitude of the relative error in Figure 6: for Raman, even a significant change of the coefficients diagonally across the black area (minimum) causes a rather small variation of the error. Note also the different scales (δ/δ_0) for Raman and ROA in Figure 6. This relative insensitivity of Raman scattering to conformation change, combined with the limited accuracy of the simulations, can cause a large dispersion of conformer ratios, as apparent in Figure 5. On the other hand, Raman spectra can be measured with higher precision[3] and calculated more reliably[68] than ROA. The overall performance of the spectroscopic–theoretical determination of conformer ratios is thus variable for a particular system and depends on a number of factors, including the theoretical model employed and experimental conditions. For Ala-Ala, the advantages of ROA spectroscopy slightly prevailed.

CONCLUSIONS

We used the Ala-Ala molecule as a peptide model to understand how Raman and ROA spectral intensities relate to chemical structure and conformation. The results were verified on variously protonated and deuterated Ala-Ala forms. The flexibility of the molecule and strong interaction with the aqueous environment made it necessary to perform rather extensive, combined molecular dynamics and quantum mechanical simulations. A very good agreement has been achieved between simulated and experimental spectra,

DOI: 10.1021/acs.jpcb.7b07154
J. Phys. Chem. B 2017, 121, 8956–8964

ultimately enabling a quantitative decomposition of the experimental data into the calculated spectral curves. Still, some spectral features were not explicable within feasible computational methodology, in particular the DFT and harmonic approximations, which needs to be addressed in the future. The explicit treatment of the water environment by molecular dynamics was of critical importance for the simulations of the peptide geometry and spectra to be realistic.

We took advantage of the good quality of calculated results to extract experimental conformer populations by a direct decomposition of experimental spectra into simulated conformer subspectra. Obtained conformer ratios roughly corresponded to results predicted by molecular dynamics, except for the content of the α-helical-like conformer in the protonated peptide, which was significantly overestimated by MD. Systematic mapping of the coefficient space revealed a good numerical stability of the spectral decomposition and enabled its optimization. Overall, we find the structure and conformer determination based on the spectroscopic and theoretical methodology to be a robust procedure, with immense potential for biomolecular studies.

■ ASSOCIATED CONTENT

Supporting Information

The Supporting Information is available free of charge on the ACS Publications website at DOI: 10.1021/acs.jpcb.7b07154.

Further computational details and characterizations of the synthesized compounds (PDF)

■ AUTHOR INFORMATION

Corresponding Authors

*E-mail: kapitan@optics.upol.cz.
*E-mail: bour@uochb.cas.cz.

ORCID

Petr Bouř: 0000-0001-8469-1686

Notes

The authors declare no competing financial interest.

■ ACKNOWLEDGMENTS

The work was supported by the Grant Agency (16-05935S) and Ministry of Education (LTC17012 and COST Action CA15214) of the Czech Republic. A large part of the computations was performed at the National Grid Infrastructure (Metacentrum, CESNET program LM2015042). We thank Dr. Radek Pelc (Stentor Institute) for the comments on the manuscript.

■ REFERENCES

(1) Hug, W. Virtual Enantiomers as the Solutuion of Optical Activity's Deterministic Offset Problem. *Appl. Spectrosc.* **2003**, *57*, 1−13.

(2) Barron, L. D. *Molecular Light Scattering and Optical Activity*; Cambridge University Press: Cambridge, U.K., 2004.

(3) Nafie, L. *Vibrational Optical Activity: Principles and Applications*; Wiley: Chichester, U.K., 2011.

(4) Zhu, F. J.; Isaacs, N. W.; Hecht, L.; Barron, L. D. Raman Optical Activity: A Tool for Protein Structure Analysis. *Structure* **2005**, *13*, 1409−1419.

(5) Johannessen, C.; Pendrill, R.; Widmalm, G.; Hecht, L.; Barron, L. D. Glycan Structure of a High-Mannose Glycoprotein from Raman Optical Activity. *Angew. Chem., Int. Ed.* **2011**, *50*, 5349−5351.

(6) Barron, L. D. The Development of Biomolecular Raman Optical Activity Spectroscopy. *Biomed. Spectrosc. Imaging* **2015**, *4*, 223−253.

(7) Weymuth, T.; Reiher, M. Characteristic Raman Optical Activity Signatures of Protein B-Sheets. *J. Phys. Chem. B* **2013**, *117*, 11943−11953.

(8) Parchaňský, V.; Kapitán, J.; Bouř, P. Inspecting Chiral Molecules by Raman Optical Activity Spectroscopy. *RSC Adv.* **2014**, *4*, 57125−57136.

(9) Eker, F.; Cao, X.; Nafie, L.; Schweitzer-Stenner, R. Tripeptides Adopt Stable Structures in Water. A Combined Polarized Visible Raman, FTIR, and VCD Spectroscopy Study. *J. Am. Chem. Soc.* **2002**, *124*, 14330−14341.

(10) Polavarapu, P. L.; Nafie, L. Vibrational Optical Activity: Comparison of Theoretical and Experimental Results for (+)-(3R)-Methylcyclohexanone. *J. Chem. Phys.* **1980**, *73*, 1567−1575.

(11) Ruud, K.; Helgaker, T.; Bouř, P. Gauge-Origin Independent Density-Functional Theory Calculations of Vibrational Raman Optical Activity. *J. Phys. Chem. A* **2002**, *106*, 7448−7455.

(12) Ruud, K.; Thorvaldsen, J. Theoretical Approaches to the Calculation of Raman Optical Activity Spectra. *Chirality* **2009**, *21*, E54−E67.

(13) Cheeseman, J. R.; Frisch, M. J. Basis Set Dependence of Vibrational Raman and Raman Optical Activity Intensities. *J. Chem. Theory Comput.* **2011**, *7*, 3323−3334.

(14) Liegeois, V.; Ruud, K. Champagne, B. An Analytical Derivative Procedure for the Calculation of Vibrational Raman Optical Activity Spectra. *J. Chem. Phys.* **2007**, *127*, 204105.

(15) Luber, S.; Reiher, M. Theoretical Raman Optical Activity Study of the B Domain of Rat Metallothionein. *J. Phys. Chem. B* **2010**, *114*, 1057−1063.

(16) Jovan Jose, K. V.; Raghavachari, K. Raman Optical Activity Spectra for Large Molecules through Molecules-in-Molecules Fragment-Based Approach. *J. Chem. Theory Comput.* **2016**, *12*, 585−594.

(17) Yamamoto, S.; Li, X.; Ruud, K.; Bouř, P. Transferability of Various Molecular Property Tensors in Vibrational Spectroscopy. *J. Chem. Theory Comput.* **2012**, *8*, 977−985.

(18) Kessler, J.; Kapitán, J.; Bouř, P. First-Principles Predictions of Vibrational Raman Optical Activity of Globular Proteins. *J. Phys. Chem. Lett.* **2015**, *6*, 3314−3319.

(19) Choi, J. H.; Cho, M. H.; Amide, I. Raman Optical Activity of Polypeptides: Fragment Approximation. *J. Chem. Phys.* **2009**, *130*, 014503.

(20) Hopmann, K. H.; Ruud, K.; Pecul, M.; Kudelski, A.; Dračínský, M.; Bouř, P. Explicit Versus Implicit Solvent Modeling of Raman Optical Activity Spectra. *J. Phys. Chem. B* **2011**, *115*, 4128−4137.

(21) Parchaňský, V.; Kapitán, J.; Kaminský, J.; Šebestík, J.; Bouř, P. Ramachandran Plot for Alanine Dipeptide as Determined from Raman Optical Activity. *J. Phys. Chem. Lett.* **2013**, *4*, 2763−2768.

(22) Melcrová, A.; Kessler, J.; Bouř, P.; Kaminský, J. Simulation of Raman Optical Activity of Multi-Component Monosaccharide Samples. *Phys. Chem. Chem. Phys.* **2016**, *18*, 2130−2142.

(23) Buděšínský, M.; Daněček, P.; Bednárová, L.; Kapitán, J.; Baumruk, V.; Bouř, P. Comparison of Quantitative Conformer Analyses by Nuclear Magnetic Resonance and Raman Optical Activity Spectra for Model Dipeptides. *J. Phys. Chem. A* **2008**, *112*, 8633−8640.

(24) Barron, L. D.; Buckingham, A. D. Simple Two-Group Model for Rayleigh and Raman Optical Activity. *J. Am. Chem. Soc.* **1974**, *96*, 4769−4773.

(25) Herrmann, C.; Ruud, K.; Reiher, M. Can Raman Optical Activity Separate Axial from Local Chirality? A Theoretical Study of Helical Deca-Alanine. *ChemPhysChem* **2006**, *7*, 2189−2196.

(26) Yamamoto, S.; Furukawa, T.; Bouř, P.; Ozaki, Y. Solvated States of Poly-L-Alanine α-Helix Explored by Raman Optical Activity. *J. Phys. Chem. A* **2014**, *118*, 3655−3662.

(27) Oboodi, M. R.; Alva, C.; Diem, M. Solution Phase Raman Studies of Alanyl Dipeptides and Various Isotopomers. A Reevaluation of Accepted Amide Vibrational Frequencies. *J. Phys. Chem.* **1984**, *88*, 501−505.

(28) Yu, G. S.; Freedman, T. B.; Nafie, L. A.; Deng, Z. Y.; Polavarapu, P. L. Experimental Measurement and Ab Initio Calculation of Raman

DOI: 10.1021/acs.jpcb.7b07154
J. Phys. Chem. B 2017, 121, 8956−8964

Optical Activity of L-Alanine and Its Deuterated Isotopomers. *J. Phys. Chem.* **1995**, *99*, 835−843.
(29) Welch, W. R. W.; Kubelka, J.; Keiderling, T. A. Infrared, Vibrational Circular Dichroism, and Raman Spectral Simulations for β-Sheet Structures with Various Isotopic Labels, Interstrand, and Stacking Arrangements Using Density Functional Theory. *J. Phys. Chem. B* **2013**, *117*, 10343−10358.
(30) Lakhani, A.; Roy, A.; De Poli, M.; Nakaema, M.; Formaggio, F.; Toniolo, C.; Keiderling, T. A. Experimental and Theoretical Spectroscopic Study of 3(10)-Helical Peptides Using Isotopic Labeling to Evaluate Vibrational Coupling. *J. Phys. Chem. B* **2011**, *115*, 6252−6264.
(31) Lucas, B.; Gregoire, H.; Maitre, P.; Ortega, J. M.; Rupenyan, A.; Reimann, B.; Scherman, J. P.; Desfrancois, C. Investigation of the Protonation Site in the Dialanine Peptide by Infrared Multiphoton Dissociation Spectroscopy. *Phys. Chem. Chem. Phys.* **2004**, *6*, 2659−2663.
(32) Šebek, J.; Gyurscik, B.; Šebestík, J.; Kejík, Z.; Bernárová, L.; Bouř, P. Interpretation of Synchrotron Radiation Circular Dichroism Spectra of Anionic, Cationic, and Zwitterionic Dialanine Forms. *J. Phys. Chem. A* **2007**, *111*, 2750−2760.
(33) Yu, G. S.; Che, D. P.; Freedman, T. B.; Nafie, L. A. Raman Optical-Activity of Simple Alanyl Peptides - Backscattering in-Phase Dual Circular-Polarization Measurements in Aqueous-Solution. *Biospectroscopy* **1995**, *1*, 113−123.
(34) Knapp-Mohammady, M.; Jalkanen, K. J.; Nardi, F.; Wade, R. C.; Suhai, S. L-Alanyl-L-Alanine in the Zwitterionic State: Structures Determined in the Presence of Explicit Water Molecules and with Continuum Models Using Density Functional Theory. *Chem. Phys.* **1999**, *240*, 63−77.
(35) Sreerama, N.; Woody, R. W. Circular Dichroism of Peptides and Proteins. In *Circular Dichroism Principles and Applications*; Nakanishi, K., Berova, N., Woody, R. W., Eds.; Wiley-VCH: New York, 2000; pp 601−620.
(36) Fletterick, R. J.; Tsai, C.; Hughes, R. E. The Crystal and Molecular Structure of L-Alanyl-L-Alanine. *J. Phys. Chem.* **1971**, *75*, 918−922.
(37) Zuk, W. M.; Freedman, T. B.; Nafie, L. A. Vibrational CD Studies of the Solution Conformation of Simple Alanyl Peptides as a Function of pH. *Biopolymers* **1989**, *28*, 2025−2044.
(38) Weir, A. F.; Lowrey, A. H.; Williams, R. W. Scaled Quantum Mechanical Force Field for Alanyl-Alanine Peptide in Solution. *Biopolymers* **2001**, *58*, 577−591.
(39) Jalkanen, K. J.; Nieminen, R. M.; Knapp-Mohammady, M.; Suhai, S. Vibrational Analysis of Various Isotopomers of L-Alanyl-L-Alanine in Aqueous Solution: Vibrational Absorption, Vibrational Circular Dichroism, Raman, and Raman Optical Activity Spectra. *Int. J. Quantum Chem.* **2003**, *92*, 239−259.
(40) Sychrovský, V.; Buděšínský, M.; Benda, L.; Špirko, V.; Vokáčová, Z.; Šebestík, J.; Bouř, P. Dependence of the L-Alanyl-L-Alanine Conformation on Molecular Charge Determined from Ab Initio Computations and NMR Spectra. *J. Phys. Chem. B* **2008**, *112*, 1796−1805.
(41) Šebek, J.; Kapitán, J.; Šebestík, J.; Baumruk, V.; Bouř, P. L-Alanyl-L-Alanine Conformational Changes Induced by pH as Monitored by the Raman Optical Activity Spectra. *J. Phys. Chem. A* **2009**, *113*, 7760−7768.
(42) Bouř, P.; Kapitán, J.; Baumruk, V. Simulation of the Raman Optical Activity of L-Alanyl-L-Alanine. *J. Phys. Chem. A* **2001**, *105*, 6362−6368.
(43) Šugar, J.; Bouř, P. Quantitative Analysis of Sugar Composition in Honey Using 532 nm Excitation Raman and Raman Optical Activity Spectra. *J. Raman Spectrosc.* **2016**, *47*, 1298−1303.
(44) Bouř, P.; Buděšínský, M.; Špirko, V.; Kapitán, J.; Šebestík, J.; Sychrovský, V. A Complete Set of NMR Chemical Shifts and Spin-Spin Coupling Constants for L-Alanyl-L-Alanine Zwitterion and Analysis of Its Conformational Behavior. *J. Am. Chem. Soc.* **2005**, *127*, 17079−17089.
(45) Hug, W.; Hangartner, G. A Novel High-Throughput Raman Spectrometer for Polarization Difference Measurements. *J. Raman Spectrosc.* **1999**, *30*, 841−852.
(46) Case, D. A.; Cheatham, I. T. E.; Darden, T.; Gohlke, H.; Luo, R.; Merz, J. K. M.; Onufriev, A.; Simmerling, C.; Wang, B.; Woods, R. The Amber Biomolecular Simulation Programs. *J. Comput. Chem.* **2005**, *26*, 1668−1688.
(47) Best, R. B.; Hummer, G. Optimized Molecular Dynamics Force Fields Applied to the Helix−Coil Transition of Polypeptides. *J. Phys. Chem. B* **2009**, *113*, 9004−9015.
(48) Kumar, S.; Bouzida, D.; Swendsen, R. H.; Kollman, P. A.; Rosenberg, J. M. The Weighted Histogram Analysis Method for Free-Energy Calculations on Biomolecules. I. The Method. *J. Comput. Chem.* **1992**, *13*, 1011−1021.
(49) Sellers, H. L.; Klimkowski, V. J.; Schäfer, L. Normal Coordinate Ab Initio Force Relaxation. *Chem. Phys. Lett.* **1978**, *58*, 541−544.
(50) Bouř, P.; Keiderling, T. A. Partial Optimization of Molecular Geometry in Normal Coordinates and Use as a Tool for Simulation of Vibrational Spectra. *J. Chem. Phys.* **2002**, *117*, 4126−4132.
(51) Hudecová, J.; Hopmann, K. H.; Bouř, P. Correction of Vibrational Broadening in Molecular Dynamics Clusters with the Normal Mode Optimization Method. *J. Phys. Chem. B* **2012**, *116*, 336−342.
(52) Frisch, M. J.; Trucks, G. W.; Schlegel, H. B.; Scuseria, G. E.; Robb, M. A.; Cheeseman, J. R.; Scalmani, G.; Barone, V.; Mennucci, B.; Petersson, G. A.; et al. *Gaussian 09*, revision D01; Gaussian, Inc.: Wallingford, CT, 2009.
(53) Klamt, A. COSMO and COSMO-RS. In *The Encyclopedia of Computational Chemistry*; Schleyer, P. R., Allinger, N. L., Clark, T., Gasteiger, J., Kollman, P. A., Schaefer, H. F., III, Schreiner, P. R., Eds.; John Wiley & Sons: Chichester, U.K., 1998; Vol. *1*, pp 604−615.
(54) Cances, E.; Mennucci, B.; Tomasi, J. A New Integral Equation Formalism for the Polarizable Continuum Model: Theoretical Background and Applications to Isotropic and Anisotropic Dielectrics. *J. Chem. Phys.* **1997**, *107*, 3032−3041.
(55) Berova, N.; Polavarapu, P. L.; Nakanishi, K.; Woody, R. W. *Comprehensive Chiroptical Spectroscopy, Applications in Stereochemical Analysis of Synthetic Compounds, Natural Products and Biomolecules*; Wiley: Hoboken, NJ, 2012; Vol. *2*.
(56) Cornell, W. D.; Cieplak, P.; Bayly, C. I.; Gould, I. R.; Merz, K. M.; Ferguson, D. M.; Spellmeyer, D. C.; Fox, T.; Caldwell, J. W.; Kollman, P. A. A Second Generation Force Field for the Simulation of Proteins, Nucleic Acids, and Organic Molecules. *J. Am. Chem. Soc.* **1995**, *117*, 5179−5197.
(57) Wang, J.; Cieplak, P.; Kollman, P. A. How Well Does a Restrained Electrostatic Potential (RESP) Model Perform in Calculating Conformational Energies of Organic and Biological Molecules? *J. Comput. Chem.* **2000**, *21*, 1049−1074.
(58) Foloppe, N.; MacKerell, A. D. All-Atom Empirical Force Field for Nucleic Acids: I. Parameter Optimization Based on Small Molecule and Condensed Phase Macromolecular Target Data. *J. Comput. Chem.* **2000**, *21*, 86−104.
(59) Duan, Y.; Wu, C.; Chowdhury, S.; Lee, M. C.; Xiong, G. M.; Zhang, W.; Yang, R.; Cieplak, P.; Luo, R.; Lee, T.; Caldwell, J.; Wang, J. M.; Kollman, P. A Point-Charge Force Field for Molecular Mechanics Simulations of Proteins Based on Condensed-Phase Quantum Mechanical Calculations. *J. Comput. Chem.* **2003**, *24*, 1999−2012.
(60) Elstner, M.; Jalkanen, K. J.; Knapp-Mohammady, M.; Frauenheim, T.; Suhai, S. DFT Studies on Helix Formation in N-Acetyl-(L-Alanyl)(N)-N ′-Methylamide for N = 1−20. *Chem. Phys.* **2000**, *256*, 15−27.
(61) Bouř, P.; Michalík, D.; Kapitán, J. Empirical Solvent Correction for Multiple Amide Group Vibrational Modes. *J. Chem. Phys.* **2005**, *122*, 144501.
(62) McQuarrie, D. A. *Statistical Thermodynamics*; Harper and Row: New York, 1973.
(63) Creighton, T. E. *Proteins: Structures and Molecular Properties*, 2nd ed.; W. H. Freeman and Co.: New York, 1993.

DOI: 10.1021/acs.jpcb.7b07154
J. Phys. Chem. B 2017, 121, 8956−8964

(64) Dukor, R. K.; Keiderling, T. A. Reassessment of the Random Coil Conformation: Vibrational CD Study of Proline Oligopeptides and Related Polypeptides. *Biopolymers* **1991**, *31*, 1747−1761.
(65) Hug, W. Optical Artefacts and Their Control in Raman Circular Difference Scattering Measurements. *Appl. Spectrosc.* **1981**, *35*, 115−124.
(66) Ford, S. J.; Wen, Z. Q.; Hecht, L.; Barron, L. D. Vibrational Raman Optical Activity of Alanyl Peptide Oligomers: A New Perspective on Aqueous Solution Conformation. *Biopolymers* **1994**, *34*, 303−131.
(67) Pecul, M.; Ruud, K. Ab Initio Calculation of Vibrational Raman Optical Activity. *Int. J. Quantum Chem.* **2005**, *104*, 816−829.
(68) Reiher, M.; Liegeois, V.; Ruud, K. Basis Set and Density Functional Dependence of Vibrational Raman Optical Activity Calculations. *J. Phys. Chem. A* **2005**, *109*, 7567−7574.
(69) Prampolini, G.; Livotto, P. R.; Cacelli, I. Accuracy of Quantum Mechanically Derived Force-Fields Parameterized from Dispersion-Corrected DFT Data: The Benzene Dimer as a Prototype for Aromatic Interactions. *J. Chem. Theory Comput.* **2015**, *11*, 5182−5196.
(70) Cortez, M. H.; Brinkmann, N. R.; Polik, W. F.; Taylor, P. R.; Bomble, Y. J.; Stanton, J. F. Factors Contributing to the Accuracy of Harmonic Force Field Calculations for Water. *J. Chem. Theory Comput.* **2007**, *3*, 1267−1274.
(71) Crawford, T. D.; Ruud, K. Coupled-Cluster Calculations of Vibrational Raman Optical Activity Spectra. *ChemPhysChem* **2011**, *12*, 3442−3448.
(72) Brancato, G.; Rega, N.; Barone, V. A Hybrid Explicit/Implicit Solvation Model for First Principle Molecular Dynamics Simulations in Condensed Phase. *J. Chem. Phys.* **2008**, *128*, 144501.
(73) Carbonniere, P.; Lucca, T.; Pouchan, C.; Rega, N.; Barone, V. Vibrational Computations Beyond the Harmonic Approximation: Performances of the B3LYP Density Functional for Semirigid Molecules. *J. Comput. Chem.* **2005**, *26*, 384−388.
(74) Daněček, P.; Kapitán, J.; Baumruk, V.; Bednárová, L.; Kopecký, V., Jr.; Bouř, P. Anharmonic Effects in IR, Raman and Raman Optical Activity Spectra of Alanine and Proline Zwitterions. *J. Chem. Phys.* **2007**, *126*, 224513.

DOI: 10.1021/acs.jpcb.7b07154
J. Phys. Chem. B 2017, 121, 8956−8964